

## Kinetic Roughening of Ion-Sputtered Pd(001) Surface: Beyond the Kuramoto-Sivashinsky Model

T. C. Kim,<sup>1</sup> C.-M. Ghim,<sup>2,\*</sup> H. J. Kim,<sup>1</sup> D. H. Kim,<sup>1</sup> D. Y. Noh,<sup>1</sup> N. D. Kim,<sup>3</sup> J. W. Chung,<sup>3</sup> J. S. Yang,<sup>4</sup> Y. J. Chang,<sup>4</sup>  
T. W. Noh,<sup>4</sup> B. Kahng,<sup>2</sup> and J.-S. Kim<sup>5,†</sup>

<sup>1</sup>Department of Materials Science and Engineering, Gwangju Institute of Science and Technology, Gwangju, 500-712, Korea

<sup>2</sup>School of Physics and Center for Theoretical Physics, Seoul National University, Seoul 151-747, Korea

<sup>3</sup>Department of Physics and BSRI, Pohang University of Science and Technology,  
Pohang 790-784, Korea

<sup>4</sup>School of Physics and Research Center for Oxide Electronics, Seoul National University, Seoul 151-747, Korea

<sup>5</sup>Department of Physics, Sook-Myung Women's University, Seoul 140-742, Korea

(Received 3 September 2003; revised manuscript received 10 February 2004; published 17 June 2004)

We investigate the kinetic roughening of Ar<sup>+</sup> ion-sputtered Pd(001) surface both experimentally and theoretically. *In situ* real-time x-ray reflectivity and *in situ* scanning tunneling microscopy show that nanoscale adatom islands form and grow with increasing sputter time  $t$ . Surface roughness  $W(t)$  and lateral correlation length  $\xi(t)$  follow the scaling laws  $W(t) \sim t^\beta$  and  $\xi(t) \sim t^{1/z}$  with the exponents  $\beta \approx 0.20$  and  $1/z \approx 0.20$ , for an ion beam energy  $\varepsilon = 0.5$  keV, which is inconsistent with the prediction of the Kuramoto-Sivashinsky (KS) model. We thereby extend the KS model by applying the coarse-grained continuum approach of the Sigmund theory to the order of  $\mathcal{O}(\nabla^4, h^2)$ , where  $h$  is the surface height, and derive a new term of the form  $\nabla^2(\nabla h)^2$  which plays a decisive role in describing the observed morphological evolution of the sputtered surface.

DOI: 10.1103/PhysRevLett.92.246104

PACS numbers: 68.55.-a, 05.45.-a, 64.60.Cn, 79.20.Rf

Recently, the observation of ordered nanostructures such as ripples and two-dimensional patterns on ion-sputtered surfaces has attracted much attention due to the demonstration of the possibility of fabrication of ordered nanoscale structures in a relatively easy and affordable way [1–3]. Such experimental results have motivated extensive theoretical investigations. A linear model, proposed by Bradley and Harper (BH) [4], has been successful in predicting the formation of the ripple structure. The wavelength, orientation, and amplitude of the ripples can be predicted in terms of experimental parameters such as the incident angle of the ion beam and substrate temperature [5]. The BH theory, however, fails to explain a number of experimental observations such as the saturation of the ripple amplitude [6] or the appearance of kinetic roughening [7,8]. To remedy such shortcomings, the noisy Kuramoto-Sivashinsky (KS) equation [9] was introduced based on the Sigmund theory of sputter erosion [10]. In addition to the linear terms of the BH model, it contains a nonlinear term proportional to  $(\nabla h)^2$ , known as the Kardar-Parisi-Zhang (KPZ) term [11], where  $h$  is surface height. Because of the nonlinear term, the surface roughness or ripple amplitude is asymptotically saturated into a constant value [12].

Kinetic roughening behavior is described by the scaling theory [13]. The surface roughness of the sample,  $L \times L$  in size, at sputter time  $t$  is defined as  $W \equiv \sqrt{(1/L^2) \sum_{\mathbf{r}} [h(\mathbf{r}, t) - \bar{h}]^2}$ , where  $\bar{h} = (1/L^2) \sum_{\mathbf{r}} h(\mathbf{r}, t)$ . It follows the scaling relation,  $W(L, t) \sim L^\alpha g(t/L^{\alpha/\beta})$ , where  $g(u) \sim u^\beta$  for  $u \ll 1$  and  $g(u \rightarrow \infty) \sim \text{const}$ . The roughness and growth exponents  $\alpha$  and  $\beta$  are related via

scaling relations to give the dynamic exponent,  $z = \alpha/\beta$ , which determines the scaling of the saturation time with the system size  $L$ . Below, we deal with the inverse dynamic exponent,  $1/z$ , called the coarsening exponent, in analyzing the experimental results.

In this Letter, we study the kinetic roughening of the sputter-eroded Pd(001) surface via novel experimental techniques combined with the stochastic continuum theory. Both *in situ* real-time x-ray reflectivity (XRR) and *in situ* scanning tunneling microscopy (STM) show that nanoscale islands are formed on the surface, evolving with increasing sputter time  $t$  following the scaling function  $W(L, t)$ . In particular, we obtain  $\beta \approx 0.2$  and  $1/z \approx 0.2$  for ion beam energy  $\varepsilon = 0.5$  keV, which are neither in agreement with the KS values,  $\beta_{\text{KS}} \approx 0.22\text{--}0.25$  and  $1/z_{\text{KS}} \approx 0.25\text{--}0.33$  [14], nor with the KPZ values,  $\beta_{\text{KPZ}} \approx 0.25$  and  $1/z_{\text{KPZ}} \approx 0.63$  [13]. To resolve this inconsistency, we investigate theoretically the erosion process by applying the Sigmund theory to higher order, finding that the relevant higher order term is of the form  $\nabla^2(\nabla h)^2$ , referred to as the conserved KPZ (CKPZ) term. In fact, preceding studies anticipated the CKPZ term induced by the instability at step edges [15,16]. However, there has been no explicit derivation thereof starting from the microscopic nature of sputter erosion. Thus, the coefficient was also not to be derived from experimental parameters, but only has been given *ad hoc*. Here applying the Sigmund theory, we derive the CKPZ term and the coefficient as well explicitly in terms of experimental parameters, which enables us to directly assess the theoretical predictions against experimental results.

**Experiment.**—A Pd(001) sample was cleaned by several cycles of Ar<sup>+</sup> ion sputtering around 300 K and annealing up to 920 K. The clean Pd(001) surface exhibited an average terrace size of about 3000 Å and little surface modulation or defects by contaminants as judged by STM images. The initial surface roughness of the sample was less than 2 Å, and the miscut from surface normal direction was 0.3°, as determined, respectively, by XRR and x-ray diffraction spot-profile analysis. Sputtering experiments were performed for Pd(001) around 300 K with Ar<sup>+</sup> ion beam incident normally to the sample surface. To avoid possible contamination during sputtering, fresh Ar gas (purity of 99.999%) was continuously made to flow through the chamber with Ar partial pressure maintained around  $2.0 \times 10^{-5}$  Torr.

The morphological evolution of the Pd(001) during sputtering was observed *in situ* by both XRR and STM. The XRR experiment was performed in a custom-designed UHV chamber at the 5C2 GIST beamline of the Pohang Light Source in Korea. The base pressure of the chamber was kept below mid- $10^{-10}$  Torr. The incident x rays were vertically focused by a mirror to 1 mm in size, and a double-bounce Si(111) monochromator was employed to both focus the beam in the horizontal direction and monochromatize the incident x ray to a wavelength of 1.24 Å, which corresponded to the x-ray energy of 10 keV. The x-ray reflectivity was measured in real time while Pd(001) was sputtered. The incident Ar<sup>+</sup> beam energy,  $\varepsilon$ , ranged from 0.5 to 2.0 keV, and the ion beam flux,  $f$ , measured from the ion current collected at the sample, ranged from  $0.5 \times 10^{13}$  to  $2.5 \times 10^{13}$  ions/cm<sup>2</sup>/s. Sputtering started with the sample at room temperature measured by a thermocouple directly attached to the back end of the sample. After sputtering for more than 10 h, the sample temperature rose only less than 30 K.

To observe the sputter-induced morphological evolution in real space, a commercial STM (Omicron VT-STM) was also used. The base pressure was kept in the low  $10^{-11}$  Torr. STM tips were electrochemically etched polycrystalline W wires that were annealed and sputtered in a UHV chamber. In all the STM measurements, the tip-sample voltage was kept as 80 mV, and the tunneling current was at 1 nA with the sample at room temperature. Sputtering was performed with  $\varepsilon = 0.5$  keV and  $f = 0.5 \times 10^{13}$  ions/cm<sup>2</sup>/s. During sputtering, the sample temperature was around 300 K. Sputtering and STM measurement were alternated, and the sputter time referred to in this Letter is the total sputtering periods. X-ray reflectivity indicated that there was no significant change in the surface roughness for 10 h after the interruption of sputtering. Thus, the interruption of sputtering for the STM measurement was not expected to result in additional relaxation of the sputtered surface.

**Experimental results.**—In Born approximation, which holds above the critical angle, the specular reflectivity

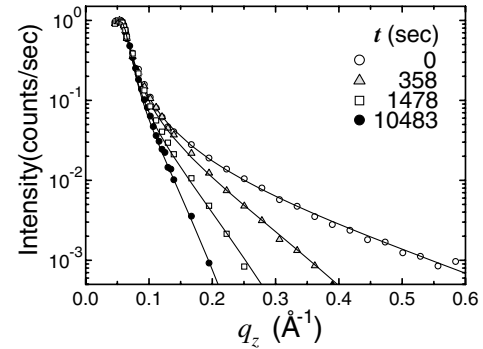


FIG. 1. Specular x-ray reflectivity (symbols) as a function of the momentum transfer,  $q_z$ , for increasing sputter times with  $\varepsilon = 0.5$  keV and  $f = 2.0 \times 10^{13}$  ions/cm<sup>2</sup>/s. The solid lines are the theoretical prediction by the Parratt formula.

decreases as  $\exp(-W^2 q_z^2)$  with increasing  $q_z$  [17]. Figure 1 shows that the reflectivity decays more steeply as the sputtering proceeds, which indicates that  $W(t)$  increases with  $t$ . Quantitatively  $W(t)$  is determined by fitting the experimental data according to the Parratt formalism [17,18]. Figure 2 shows  $W(t)$  thus obtained, as a function of  $t$  for several  $\varepsilon$  but with a fixed  $f$ . The linear behavior in double-logarithmic scale implies power-law behavior,  $W(t) \sim t^\beta$ . We obtained that  $\beta \approx 0.20 \pm 0.02$  for  $\varepsilon = 0.5$  keV,  $\beta \approx 0.23 \pm 0.02$  for  $\varepsilon = 1.5$  keV, and  $\beta \approx 0.25 \pm 0.02$  for  $\varepsilon = 2.0$  keV.

The inset of Fig. 2 summarizes the surface roughness  $W(t)$  as a function of fluence ( $f \times t$ ) for several different  $f$ 's, but with a fixed  $\varepsilon$ . We find that the roughness evolves showing the same fluence dependence, irrespective of  $f$ . Such behavior implies that the surface diffusion is not induced by thermal activation, but rather by the surface sputtering under the present experimental condition [19].

We also study the facet formation on the sputtered surface by tracing the extradiffraction peaks or satellites around the diffraction peak corresponding to the sample surface, now the (001) plane, because each facet plane defines diffraction rods normal to it. In the inset of Fig. 3,

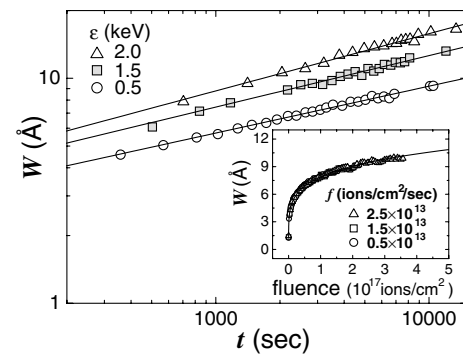


FIG. 2. The surface roughness  $W$  as a function of sputter time  $t$  for different ion energies,  $\varepsilon = 0.5$  (○), 1.5 (□), and 2.0 (△) keV, but with a fixed ionic flux,  $f = 2.0 \times 10^{13}$  ions/cm<sup>2</sup>/s. The inset shows that the roughness evolution for a given  $\varepsilon$  follows the same fluence dependence, irrespective of  $f$ .

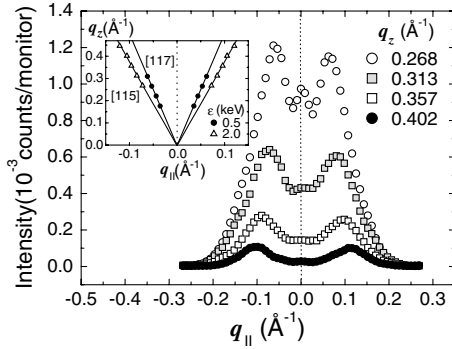


FIG. 3. X-ray diffraction intensity along [110] for different  $q_z$ . The positions of satellite peaks shift to the larger  $q_{||}$  for the larger  $q_z$ , with a fixed angle to the surface normal, indicating that the spots originate from a facet formed by sputtering. Inset: Positions of satellite peaks,  $q_{||}$ , as a function of  $q_z$ .

the diffraction rods defined by the satellite peaks make well-defined angles with respect to that of the (001) plane as much as the facet plane does to the (001) plane. From the observed angles, we identify the facet formed on sputtering by the 0.5 keV ion beam to be (117) and that by the 2.0 keV beam to be (115).

The morphological evolution of the sputtered Pd(001) surface was also investigated by an STM. Figure 4 shows the STM images of the sputtered surface at different (total) sputtering times under the same experimental condition,  $\varepsilon = 0.5$  keV and  $f = 0.5 \times 10^{13}$  ions/cm<sup>2</sup>. The shape of the island edge looks somewhat irregular, which may be due to random shot noise or the sputter-induced diffusion. This reaffirms that thermal smoothening is inefficient in the present experimental conditions as suggested by the flux-independent scaling behavior. The insets of Fig. 4 show the height-height correlation function,  $G(r, t) = \langle [h(r, t) - h(0, 0)]^2 \rangle$ , that reveals lateral order developing on the surface as sputtering proceeds.

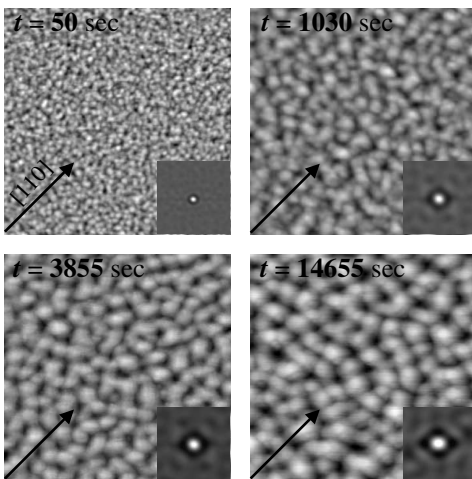


FIG. 4. STM images,  $200 \times 200$  nm<sup>2</sup> in size, according to time evolution. The insets at right bottom of each image show the height-height correlation function obtained from the corresponding surface profile.

246104-3

We can see that the island size grows with increasing sputter time. From the height-height correlation function, we determine the lateral correlation length  $\xi$  as the position giving the first-order maximum, and plot it as a function of  $t$  in Fig. 5. It is found that  $\xi \sim t^{1/z}$  with the exponent  $1/z \approx 0.20 \pm 0.03$ . The growth exponent determined by the STM measurement is  $\beta \approx 0.20 \pm 0.03$ , in agreement with that of the XRR measurement.

*Theory.*—To elucidate the kinetic roughening of the surface, we systematically expand the Sigmund theory to obtain the extended KS equation:

$$\frac{1}{c} \frac{\partial h}{\partial t} = -1 - \nu \nabla^2 h - D \nabla^4 h + \lambda_1 (\nabla h)^2 + \lambda_2 \nabla^2 (\nabla h)^2 + \eta(x, y, t), \quad (1)$$

where  $c$  is the surface recession rate given by a material constant times ionic flux,  $\nu$  the effective surface tension generated by the erosion process,  $D$  the ion-induced effective diffusion constant [19],  $\lambda_1$  and  $\lambda_2$  tilt-dependent erosion rates, and  $\eta$  uncorrelated white noise with zero mean, mimicking the randomness resulting from the stochastic nature of ion arrival at the surface. While the linear terms may have the origins of thermal diffusion and/or the Ehrlich-Schwoebel instability at step edges [20], their contributions are overwhelmed by ion-induced effects under the current experimental conditions, otherwise  $W(t)$  for various flux conditions could not collapse into a single curve [19] as shown in the inset of Fig. 2. The coefficients  $\nu$ ,  $D$ , and  $\lambda_1$  in Eq. (1) were derived in terms of empirical parameters such as ion penetration depth ( $a$ ) and cascading sizes in transverse and longitudinal directions ( $\mu$  and  $\sigma$ , respectively), which are determined experimentally by  $\varepsilon$ ,  $f$ , and the incident angle  $\theta$  for oblique incidence. The newly derived CKPZ coefficient is, under normal incidence, given by

$$\lambda_2 = \mu^2/2 + (3/8)(\mu/\sigma)^4(\sigma^2 - a^2). \quad (2)$$

Using the TRIM Monte Carlo algorithm [21], all the coefficients in Eq. (1) are determined numerically for our experimental parameters, which are tabulated in Table I. In Fig. 6 is shown the estimation of the KPZ and CKPZ

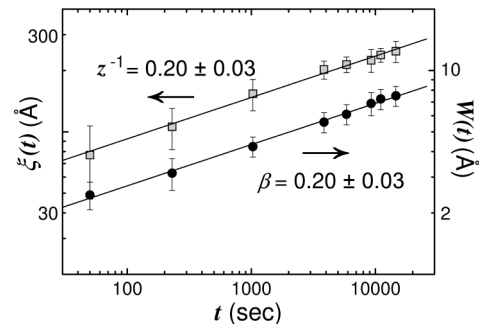


FIG. 5. Plot of the lateral correlation length  $\xi$  ( $\square$ ) and the surface roughness  $W$  ( $\bullet$ ) for  $\varepsilon = 0.5$  keV obtained from the STM images as a function of sputter time  $t$ .

246104-3

TABLE I. Numerical estimations of the coefficients in Eq. (1) under the experimental conditions we performed.

$\epsilon$	$a$ (Å)	$\nu$ (Å)	$D$ (Å <sup>3</sup> )	$\lambda_1$	$\lambda_2$ (Å <sup>2</sup> )
0.5 keV	9	2.72	33.35	-0.50	12.2
1.5 keV	16	5.12	184.32	-0.54	33.6
2.0 keV	18	5.44	266.78	-0.50	49.0

terms, for a typical profile of the eroded surface. The numerical values in Fig. 6 include the contributions from the coefficients,  $\lambda_1$  and  $\lambda_2$ , as well as from tilt-dependent terms themselves. We find that the CKPZ term should be more relevant to the morphological evolution than the KPZ term in a finite system. The contributions from other terms allowed by symmetry and of order  $\mathcal{O}(\nabla^4, h^2)$ , such as  $(\nabla^2 h)^2$ , are found to be negligible. Then, for  $\epsilon = 0.5$  keV, the extended KS equation is reduced to the CKPZ equation that gives the growth exponent  $\beta_{\text{CKPZ}} \approx 0.20$  [22] for two dimensions, in agreement with the measured value. As the ion energy increases, the coefficient  $D$  increases very rapidly in comparison with the magnitudes of  $\lambda_1$  and  $\lambda_2$  as seen in Table I. Thus, for  $\epsilon = 2.0$  keV, the erosion process is mainly governed by the so-called Mullins term,  $D\nabla^4 h$  [23]. In this case, it is known that the growth exponent  $\beta_{\text{Mullins}} \approx 0.25$  for two dimensions, again consistent with the experimental value for  $\epsilon = 2.0$  keV. The sputter-induced palladium atoms form adatom islands with well-defined facets as observed in Fig. 3. Then,  $\alpha = 1$  and the coarsening exponent,  $1/z$ , should be equal to  $\beta$  following the scaling relation  $1/z = \beta/\alpha$ . This prediction is confirmed in the present experiment by the observation of  $1/z = \beta = 0.2$  for  $\epsilon = 0.5$  keV. Furthermore, by plugging the numerical values for, say,  $\epsilon = 0.5$  keV, in Table I into Eq. (1), we estimate the typical lateral size and amplitude of islands to be  $\approx 22$  and  $3$  Å, respectively, which are compatible with the experimental results shown in Fig. 5.

**Conclusions.**—We have studied the kinetic roughening of the sputter-eroded Pd(001) surface both experimentally and theoretically. The experimental data suggest that the extended KS model with additional CKPZ term could properly describe the kinetic roughening behavior.

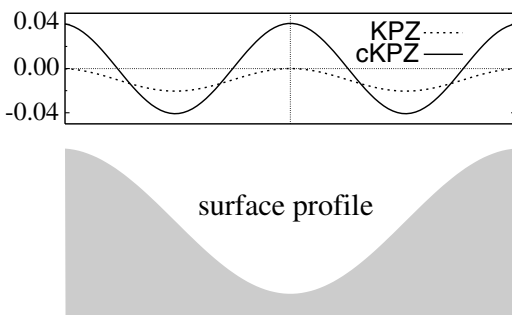


FIG. 6. Comparison of the KPZ and the CKPZ terms for a prototypical profile of eroded surface.

To this end, we apply the Sigmund theory, a coarse-grained continuum approach of collision cascade, to extract the coefficient of each term as a function of experimentally controllable parameters, which makes it possible to systematically improve our understanding of kinetic roughening on the experimental bases. We expect that the model sheds light on recent experimental realization of self-organized surface nanostructures induced by ion sputtering.

This work is supported by the KRF Grant No. 2002-015-CP0087 through SMU and KOSEF Grants No. 2002-2-11200-002-3 through SNU and No. R01-2002-000-00469-0 through GIST.

\*Electronic address: cmghim@phy.snu.ac.kr

†Electronic address: jskim@sookmyung.ac.kr

- [1] S. Facsko *et al.*, Science **285**, 1551 (1999).
- [2] F. Frost, A. Schindler, and F. Bigl, Phys. Rev. Lett. **85**, 4116 (2000).
- [3] S. Rusponi *et al.*, Phys. Rev. Lett. **81**, 2735 (1998); **81**, 4184 (1998).
- [4] R. M. Bradley and J. M. E. Harper, J. Vac. Sci. Technol. A **6**, 2390 (1988).
- [5] I. Koponen, M. Hautala, and O.-P. Sievanen, Phys. Rev. Lett. **78**, 2612 (1997).
- [6] K. Wittmaack, J. Vac. Sci. Technol. A **8**, 2246 (1990); J. Erlebacher *et al.*, Phys. Rev. Lett. **82**, 2330 (1999); J. J. Vajo *et al.*, J. Vac. Sci. Technol. A **6**, 76 (1988).
- [7] E. A. Eklund *et al.*, Phys. Rev. Lett. **67**, 1759 (1991).
- [8] H.-N. Yang, G.-C. Wang, and T.-M. Lu, Phys. Rev. B **50**, 7635 (1994).
- [9] R. Cuerno and A. L. Barabási, Phys. Rev. Lett. **74**, 4746 (1995); M. A. Makeev, R. Cuerno, and A.-L. Barabási, Nucl. Instrum. Methods Phys. Res., Sect. B **197**, 185 (2002).
- [10] P. Sigmund, Phys. Rev. **184**, 383 (1969).
- [11] M. Kardar, G. Parisi, and Y.-C. Zhang, Phys. Rev. Lett. **56**, 889 (1986).
- [12] S. Park *et al.*, Phys. Rev. Lett. **83**, 3486 (1999).
- [13] A.-L. Barabási and H. E. Stanley, *Fractal Concepts in Surface Growth* (Cambridge University Press, Cambridge, 1995).
- [14] J. T. Drotar *et al.*, Phys. Rev. E **59**, 177 (1999).
- [15] T. Michely and C. Teichert, Phys. Rev. B **50**, 11156 (1994).
- [16] S. J. Chey, J. E. Van Nostrand, and D. G. Cahill, Phys. Rev. B **52**, 16696 (1995).
- [17] S. K. Sinha *et al.*, Phys. Rev. B **38**, 2297 (1988).
- [18] L. G. Parratt, Phys. Rev. **95**, 359 (1954).
- [19] M. A. Makeev and A.-L. Barabási, Appl. Phys. Lett. **71**, 2800 (1997).
- [20] P. Politi and J. Villain, Phys. Rev. B **54**, 5114 (1996).
- [21] J. F. Ziegler, J. P. Biersack, and U. Littmark, *The Stopping and Range of Ions in Solids* (Pergamon Press, New York, 1996).
- [22] Z.-W. Lai and S. Das Sarma, Phys. Rev. Lett. **66**, 2348 (1991); S. H. Yook, J. M. Kim, and Y. Kim, Phys. Rev. E **56**, 4085 (1997).
- [23] W. W. Mullins, J. Appl. Phys. **28**, 333 (1957).